Received: 27 August 2019 | Revised: 13 January 2020 | Accepted: 14 January 2020

DOI: 10.1002/er.5210

RESEARCH ARTICLE

INTERNATIONAL JOURNAL OF ENERGY RESEARCH WILEY

Effect of storage tanks on solar-powered absorption chiller cooling system performance

Kasim Toprak[1] | **Kiswendsida E. Ouedraogo**[2]

[1]Department of Mechanical Engineering, Izmir Institute of Technology, Izmir, Turkey

[2]Department of Energy Engineering, Izmir Institute of Technology, Izmir, Turkey

Correspondence
Kasim Toprak, Department of Mechanical Engineering, Izmir Institute of Technology, Izmir 35430, Turkey.
Email: kasimtoprak@iyte.edu.tr

Summary

Thermal storage, low power tariff at night, and low nocturnal temperature can be used in synergy to reduce the cooling costs of the solar-powered absorption chiller cooling systems. This study aims to reduce the required cooling capacity of an absorption chiller (ACH) powered by a solar parabolic trough collector (PTC) and a backup fuel boiler by integrating thermal storage tanks. The thermal performance of the system is simulated for a building that is cooled for 14 h/day. The system uses 1000 m^2 PTC with 1020 kW ACH. Chilled water storage (CHWS) and cooling water storage (CWS) effects on the system performance for different operation hours per day of the ACH under Izmir (Turkey) and Phoenix (USA) weather conditions are analyzed. When the ACH operates 14 h/day as the load for both systems and both locations, the variations of the solar collector efficiency and the cooling load to heat input ratio remain less than 4% after the modifications. From the addition of CHWS to the reference system, a parametric study consisting of changing the ACH operation hours per day shows that the required cooling capacity of the ACH can be reduced to 34%. The capacity factor of the ACH is improved from its reference value of 41% up to 96%.

KEYWORDS

absorption chiller, capacity factor, thermal storage

1 | INTRODUCTION

Air conditioning (AC) is an energy-intensive process which accounts for up to 70% of building energy consumption.[1-4] Hence, the demand for renewable energy systems (RES) increases to decrease the cost of the AC bill. However, the RES such as solar, wind, and geothermal are recognized with high initial capital expenditure (CAPEX) and a low operating expenses (OPEX).[5,6] In addition to the high cost, the efficiencies and capacity factor (CF) of RES are low compared with that of fossil fuel energy systems. For example, solar plant CF is typically less than 30% and a wind turbine CF is less than 40% while a gas-fired power plant can have a CF over 90%.[7,8] To propose a more economical RES in the context of building cooling, solar thermal cooling and heating systems must be analyzed to increase their performances. The specific case of solar-powered ACH which directly converts heat into cold is investigated in this study.

Some studies have been done on the optimization of the solar-powered ACH. These optimizations include the choice of collectors' types, ACH units, and their working fluids. Among the common collector types, the parabolic trough collector (PTC) is the most efficient and economical one for location where the solar direct normal irradiation (DNI) is high, and the application requires medium temperature (100°C-300°C) fluid. On the ACH side, there are single-, multi-, and combination of double- and

single-effect ACH units. Although multi-effect ACH systems are more complex than single-effect ones, their COP values are better. However, as the number of effects increases, the ACH performance becomes negatively sensitive to the ambient temperature changes.

Besides the collector and ACH performance improvement, it is possible to boost the overall cooling system performance by integrating energy storage tanks into the systems. Storage systems that store cold or hot water have been used to increase the CF of cooling machines and reduce the CAPEX. They shift or extend the operation hours of the machines beyond the load hours or provide a thermal mass to cool down the machines (condenser and absorber). Phase change materials (PCMs) and water are the commonly used thermal storage medium.[9-11] Sivaram et al[12] developed a simple numerical model and performed experiments to investigate the performance of solar PTC integrated with thermal energy storage tank. The aperture of PTC is 7.5 m2 and the thermal energy storage has a 60-L capacity that has paraffin as PCM and water as heat transfer fluid. Their results showed that even numerical results have 10% deviations from experimental results, they reached up to 30% overall system efficiency. Due to higher cost and long-term stabilities issues of the PCMs, water is the most used material. Chilled water storage (CHWS) remains the most economical option for large systems up to 160 000 m^3.[13] A 24 000-m^3 CHWS project has been implemented to support the cooling load of Illinois University in 2011. The project achieved an 8.5-MW peak power demand reduction and enabled the school to purchase electricity during the low-power tariff hours.[14] Somkiat et al[15] conducted a similar study on performance optimization of a university cooling system in North Bangkok. Total energy consumption of the school is 13 875.5 MWh/y and AC systems use 7021.8 MWh/y of total energy. After the CHWS and operating strategies were implemented, the required chiller capacity has been reduced by 50% while the peak demand has been reduced by 31.2%. Syed et al[16] studied a solar-powered single-effect absorption chiller cooling system integrated with a hot water storage tank in Madrid through the summer period of 2003. The results showed that the cooling system continued to operate for a while after sunset and has an enhanced COP. El-Shaarawi and Al-Ugla[17] studied to investigate four different configurations of hybrid storage for a 24-hour operation of solar-powered LiBr-water absorption AC using ambient conditions of a family house in Dhahran City, Saudi Arabia that has a total daily cooling load of 120 kWh. They already stated that hybrid storage design for absorption chiller increases the performance and reduces the collector size. They also showed hybrid storage features of continuous operation and cost reduction. They compared all four models based on cost, collector area, storage capacity, and suitability for 24 hours of operation.

In the literature, the storage tank effect has been limited to peak load shifting and power saving without tackling the system size/cost reduction potential.[18-20] However, the operation sequence of the cooling or heating system that is integrated with thermal storage tanks can be optimized to have better performance. Rosiek et al[21] studied solar-assisted ACH with CHWS tank and reported 20% of the total electrical energy saving when the system operates less ON/OFF cycles. In a similar study by Zhua et al,[22] a system operation cost reduction of 20.5% was achieved. However, if the peak load of a building is shifted from daytime to nighttime in a large scale, this will lead to the same issue of huge power demand at night. A simple load shifting may be satisfying for an electric chiller, which has a relatively low specific cost. However, due to the high cost of ACH, reducing its sizes is critical for the feasibility of the project.

In this study, A MATLAB code is created to analyze the thermal performance of solar-powered absorption chiller integrated with storage tanks cooling system using the cooling load profile of a shopping center in Izmir. Initially, CHWS tanks are used to store chilled water to support the building cooling load. Then, the cooling water storage (CWS) tanks are further attached to the cooling tower to partially store warm water out of the condenser-absorber at daytime and cool it during the ACH non-operation time. The new solar systems are analyzed to learn about their capabilities to shift the base/peak cooling load of the ACH and reduce its size/cost.

2 | SYSTEMS DESCRIPTION

Three solar-powered ACH cooling systems cases are investigated. The reference is the simple solar-powered ACH system. The proposed systems integrate thermal storage tanks into the reference system. The first proposed system adds two CHWS tanks (283 m^3 each) to the reference system, while the second proposed system further adds two CWS tanks (630 m^3 each) to the first proposed system.

2.1 | Reference system (model S_0)

The simple solar-powered ACH cooling system for this study consists of a 1000-m^2 solar PTC, a 30-m^3 (V_G) hot storage tank, an 800-kW backup boiler, a 1020-kW ACH, and a cooling tower as seen in Figure 1. In this cooling system, the ACH system cools directly the building, which means that it should be sized to satisfy the maximum cooling load of the building. The required cool water of the ACH is provided with a cooling tower. The cooling

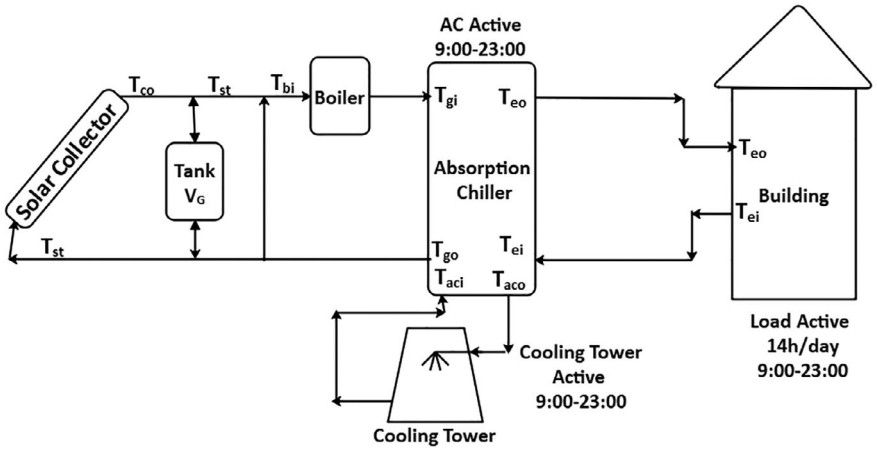

FIGURE 1 Reference cooling system, S_0

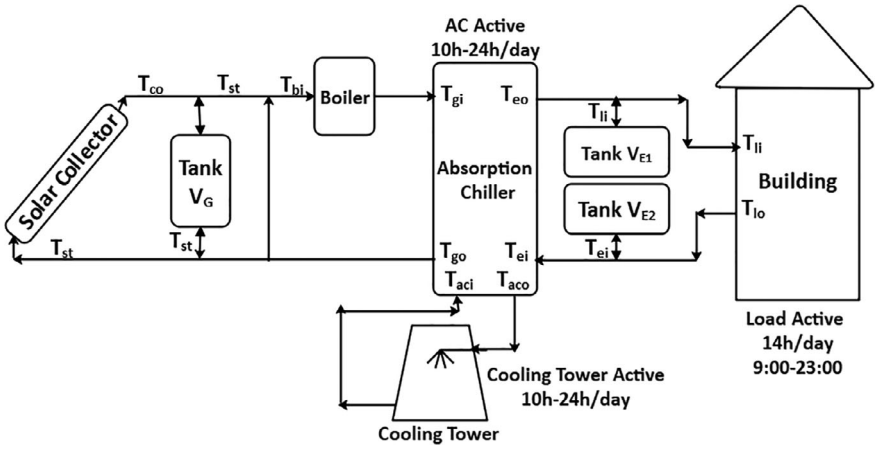

FIGURE 2 Cooling system with chilled water storage (CHWS), S_1

tower is turned ON/OFF simultaneously with the chiller. In the thermal power side of the system, solar collectors are used as a heat generator to power the system. In the case that hot water temperature is not high enough to meet the chiller requirement, a backup boiler ensures that the set temperature is reached. When the thermal hot storage tank is too hot or cold for the chiller, the hot storage tank that stores the heated water is bypassed or the hot tank water is mixed with the chiller return water to meet the required temperature.

Even though this cooling system requires an ACH with the size of the peak load of the AC space, it may be an inefficient investment in equipment as the full power of the machine may be used only a few hours a day, remaining idle the rest of the time. Also, it is worth noting that commercial buildings are often cooled less than 12 h/day, which represents a missed opportunity to increase the CF of the ACH in the reference system.

2.2 | Proposed system (model S_1)

As seen in Figure 2, the first proposed cooling system adds two CHWS tanks, V_{E1} and V_{E2}, to the reference system. When the harvested solar energy is more than the required to satisfy the cooling load, the extra energy is used to chill water (V_E) for later use. By storing chilled water in low cooling load time, the chiller rated cooling power can be reduced by using both the chiller and the stored chilled water to satisfy the cooling load during peak hours. Reducing the required chiller cooling capacity is an important point as it will reduce the initial investment as well as the operation and maintenance costs. The temperature difference between the cold tanks and the ambient temperature is certainly less than that between the hot tank and the ambient. Therefore, producing and storing chilled water causes much less heat loss compared with storing hot water for later chilled water production.

2.3 | Proposed system (model S_2)

The second proposed system is developed by integrating two CWS tanks, V_{CT1} and V_{CT2}, to the first proposed cooling system to assist the cooling tower in providing low-temperature cooling water to the ACH as shown in Figure 3. The working principle of the CWS tanks is

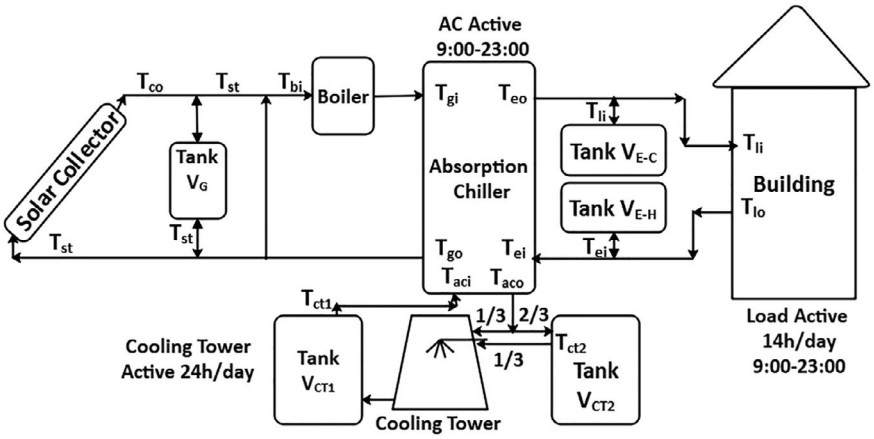

FIGURE 3 Cooling system with chilled water storage (CHWS) and cooling water storage (CWS), S_2

explained as the following. The tank V_{CT1} is full with cool water at the initial startup of the system, and as the system operates, water is drawn from the cool tank at a mass flow rate "m" to cool down the condenser and absorber of the chiller. However, from the outlet of these components, only a fraction "$1/n_{CT}$" of warm water (where $n_{CT} > 1$) is passed through the cooling tower and back to the cold tank while the remaining fraction of "$(1\text{-}1/n_{CT})$" warm water is stored in tank V_{CT2}. The fraction value, n_{CT}, the flow rate, m, and storage tank volume, V_{CT}, are calibrated so that the tank V_{CT1} is empty and the tank V_{CT2} is full at the end of chiller operation hours. The operation hours of ACH chiller is completed for a day, and warm water in V_{CT2} is cooled at a low flow rate "m/n_{CT}" to fill back the cool tank V_{CT1} for the following operation time of the ACH. In this configuration, the cooling tower always operates at a lower flow rate "m/n_{CT}" rather than intermittently at a unit flow rate m or "0" as in the reference system. It is expected that cooling water at night will take advantage of both low night temperature and low-electricity tariff to improve the performance of the system and lower the cost of consumed power.

3 | SYSTEM COMPONENTS MODELS

In this section, the mathematical models for each component are described. Since the magnitude of electrical energy consumption of pumps, fan, and monitoring devices are negligible compared with the ACH heat consumption, they are not taken into the calculations.

3.1 | Cooling load and weather data

The cooling load profile of the shopping center in Izmir, Turkey is used for this study. It is showed in Figure 4. It has been reported that because of the massive internal load and the good insulation of the building, the cooling load profile

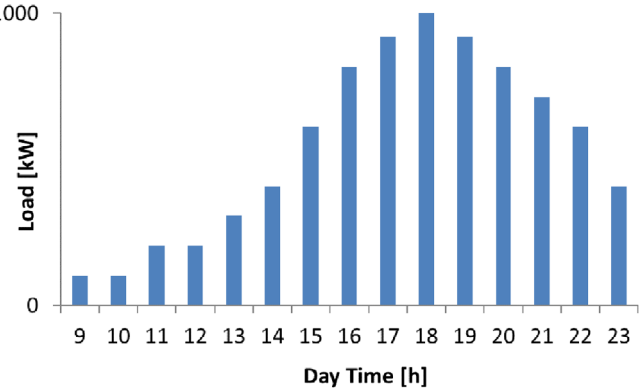

FIGURE 4 Cooling load profile of the shopping mall [Colour figure can be viewed at wileyonlinelibrary.com]

does not depend much on weather conditions.[23] For these reasons, the same load profile has been kept for the simulation of the system in Phoenix, USA to see the performance of the system in different weather conditions. It is assumed that the daily cooling load of the shopping center is unchanged for the whole summer (April to September).

Table 1 shows the typical meteorological year (TMY) data of the two cities that are obtained from TRNSYS database.[24] As seen from the weather data, Phoenix is sunnier, hotter, and drier compared with Izmir. DNI ratio for both cities reached the critical value of 60% that makes multi-effect absorption chiller usage cost-effective compared with single-effect chiller.[25] DNI value of Phoenix reaches 80%, which makes it a better place for concentrating solar thermal applications. For both locations, it is observed that nighttime dry/wet bulb temperature is less than daytime temperatures that makes night cooling an attractive.

3.2 | Solar collector

A single-axis tracking PTC is less efficient than dual-axis tracking PTC; however, due to its simplicity and lower

TABLE 1 TMY data of Izmir and Phoenix[24]

Parameters		Cities			
		Izmir		Phoenix	
Annual solar radiation [kWh/m^2/year, %]	Global radiation	2382.18		3358.62	
	Direct normal radiation	1448.46	60.80	2615.83	77.88
	Diffuse radiation DIF/DIF%	879.23	36.91	676.12	20.13
	Reflected radiation REF/REF%	879.23	2.29	66.68	1.99
Annual ambient temperature [°C]	Min/Max	−3.41	37.97	−2.94	46.17
	Average	17.06		22.53	
Annual relative humidity [%]	Min/Max	26.13	99.75	4.00	99.88
	Average	60.83		36.31	
Cooling season ambient temperature [°C]	Average day/night	25.25	21.06	32.03	26.38
Cooling season wet bulb temperature [°C]	Average day/night	17.38	15.67	18.03	16.14

Abbreviation: TMY, typical meteorological year

cost, it is still the most used in solar thermal applications. A single-axis tracking PTC from IEA SHC-TASK 33 database is used in this study. Its second-order efficiency curve function model is given by[26]

$$\eta = \eta_0 - a_1\frac{\Delta T}{DNI} - a_2\frac{\Delta T^2}{DNI}, \quad (1)$$

where $\eta_0[-]$ is the collector efficiency ($\eta_0 = 0.75$), $a_1[W/m^2K]$ is the first-order heat loss coefficient ($a_1 = 0.1123$), $a_2[W/m^2K]$ is the second-order heat loss coefficient ($a_2 = 0.00128$), ΔT [°C] is temperature difference between ambient and average collector temperature, and DNI $[W/m^2]$ is solar DNI. By changing the corresponding constants, the efficiency equation can be used for other solar collectors. Compared with flat plate collector, concentrating solar technology like PTC has lower heat loss coefficient due to the small surface area of the receiver tube. This enables to use of PTC type solar collectors for medium temperature applications. The higher heat loss coefficient of FPC makes it unsuitable for applications requiring temperature over 100°C. In Equation 2, the DNI is read normal to the collector aperture area and it is generated by using single-axis tracking is in TRNSYS. The collector efficiency is also given by the following:

$$\eta = \frac{Q_{useful}}{A_c DNI}, \quad (2)$$

$$Q_{useful} = m_{sc}C_p(T_{co} - T_{ci}), \quad (3)$$

where Q_{useful} $[W]$ is useful harvested energy from the collector, A_c $[m^2]$ is the collector aperture area, $m_{sc}[kg/s]$ is solar collector mas flow rate, $C_p[kJ/kg.C]$ is water specific heat, $T_{co}[C]$ is collector outlet temperature, and $T_{ci}[C]$ is collector inlet temperature. Equations 2 and 3 are iterated to solve for the outlet temperature of the collector. However, it should be noted that 250°C is the ceiling temperature value of the PTC for industrial heat process collectors. As a result, the testing of the collector is done for a limited temperature range. The solar fraction is the ratio of solar energy to the total energy needed to power the system. It is an important performance indicator defined as

$$sf = \frac{Q_S}{Q_S + Q_b}. \quad (4)$$

3.3 | Storage tank

The storage tanks heat losses are calculated using U value of the insulation material. The hot storage tank for the solar collector and the CHWS tanks are insulated with 10-cm thick rock wool with a U value of 0.45 W/m$^{2\circ}$C, and the CWS tanks are insulated with a 10-cm concrete block with a U value of 33 W/m$^{2\circ}$C.[27,28] From TMY data, since the average wind speed is less than 4 m/s, the thermal resistance associated with outside convective heat transfer coefficient has been neglected. To quantify the heat loss of both V_G and V_E tanks, the total heat loss term has been defined as

$$Q_{loss} = Q_{loss,VG} + \frac{Q_{loss,VE}}{COP_{chiller}}. \quad (5)$$

The heat loss in the cold tank V_E has been converted to the equivalent heat input at the generator to provide the cooling power lost.

3.4 | Absorption chiller

The absorption chiller is modeled according to its characteristic temperature function, ΔΔT, that determines the performance of the chiller using external fluid streams data. It uses the average temperatures of the three fluid streams (Generator, Evaporator, and Absorber-Condenser) to express their corresponding heat flow as well as the COP of the machine. ΔΔT is given by

$$\Delta\Delta T = T_G + aT_{AC} + eT_E, \tag{6}$$

where the constants "a" and "e" are dependents on the chiller characteristics. The cooling power Q_E, the generator power Q_G, the heat rejection rate of the absorber and condenser Q_{AC}, and the COP are then given by the following equations:

$$Q_E = s_E\Delta\Delta T + r_E, \tag{7}$$

$$Q_G = s_G\Delta\Delta T + r_G, \tag{8}$$

$$Q_{AC} = Q_E + Q_G, \tag{9}$$

$$COP = \frac{Q_E}{Q_G}. \tag{10}$$

The design conditions and characteristic coefficient of the ACH are given in Table 2. A double-effect ACH with a COP of 1.33 is preferred to a single-effect ACH with a COP of 0.7 for this building.

The total heat input per unit cooling power is defined as the system performance ratio (SPR).

$$SPR = \frac{Q_L}{Q_S + Q_b}. \tag{11}$$

Also, CF or utilization ratio of the chiller is used to measure the improvement of the system in terms of CAPEX and OPEX reduction potential. It is defined as

$$CF = \frac{\sum((\text{Cooling Load})(Load\ time))}{(\text{Chiller Rated Power})(\text{Cooling Season Duration})}. \tag{12}$$

3.5 | Cooling tower

The cooling tower calculations are performed with an induced draft counterflow-type cooling tower, and the cooling efficiency is defined by[29,30]:

TABLE 2 Absorption chiller nominal operating conditions[25]

Chiller Parameters		Characteristics Coefficients	
Chilled water in/out [°C]	**14/7**	***a***	**−2.46**
Cooling water in/out [°C]	30/37	*e*	4.38
Hot water out/in [°C]	180/165	s_E	18.1
Chilled water flow rate [m^3/h]	143	r_E	−1350.5
Cooling water flow rate [m^3/h]	244	s_G	12.54
Hot water flow rate [m^3/h]	51	r_G	−917.3
Cooling capacity [kW]	1163		
COP [−]	1.33		

$$\varepsilon = \frac{T_{inh} - T_{outc}}{T_{inh} - T_{wb}}. \tag{13}$$

However, since the efficiency and the outlet temperature are unknown, a correlation detailed by Mansour et al[31] is used to calculate the CT efficiency as follows:

$$\varepsilon = \frac{\varepsilon^*}{\varepsilon^* + 1}, \tag{14}$$

$$\varepsilon^* = \frac{(Cro)(NTU)}{1 - 0.5NTU\left(Cro - \frac{L}{G}\right)}, \tag{15}$$

$$NTU = c\left(\frac{L}{G}\right)^{n+1}, \tag{16}$$

$$Cro = \frac{b}{C_p}. \tag{17}$$

The L/G parameter stands for the water-air mass flow ratio. Liu et al[29] and Khamis et al[31] studied the counter flow cooling tower and obtained an optimal L/G ratio of 0.83, which is used in this study. The constants "c" and "n" are characteristics of the cooling tower which depend on the geometry of the tower and the roughness of the fill material. Typical values of c ranges from 1.5 to 4, while that of n ranges from −0.4 to −0.8. The CT used by Liu et al[29] with c = 4 and n = −0.72 is selected for this study. The term "b" is the slope coefficient of the saturated water enthalpy as a function of wet bulb temperature.

3.6 | Flow process

The thermal storage tanks are integrated with the cooling systems and enable to manipulate the water flow rates of both cooling tower and chiller. The volumes of the tanks

are calibrated along with the mass flow rates and operation time to unsure that cool water is always available for the ACH.

The CT of the reference system and the first proposed system operates during active hours along with ACH at a mass flow rate of m_{ac}. On the other hand, the CT of the second proposed system works continuously at a reduced mass flow rate of m_{ac}/n_{CT}. At the end of the cooling hour of ACH, CWS tanks V_{CT1} is empty and V_{CT2} is full with warm water. Water in tank V_{CT2} is cooled and transferred to the tank V_{CT1} during the OFF time, ΔT_{OFF}, as expressed in Equation 18.

$$M_{ac_{OFF}} = \frac{1}{n_{CT}} m_{ac} \Delta t_{OFF}, \tag{18}$$

$$m_{ac} \Delta t_{ON} = M_{ac_{ON}} + \frac{1}{n_{CT}} m_{ac} \Delta t_{ON}. \tag{19}$$

At the start of the ON time cycle, V_{CT1} is full and V_{CT2} is empty. Water used by the ACH during the ON time cycle is the summation of water in tank V_{CT1} at the beginning of the chiller operation and cooled water during ΔT_{ON} cycle as expressed in Equation 19. Since the amount of mass that tanks V_{CT1} and V_{CT2} can have are the same, Equations 18 and 19 are solved simultaneously to find the flow splitting term n_{CT}. The summation of ΔT_{ON} and ΔT_{OFF} is 24 hours.

4 | RESULTS AND DISCUSSION

Figure 5 shows the results of the fluid stream temperature in the generator and hot storage tank temperature for both Izmir and Phoenix. The generator temperatures of both locations follow the same pattern through the weeks and decreases as the system is integrated with thermal storage tanks. In addition to the CHWS lowers the generator temperature, adding the CWS tanks further lower the temperature. Since the CHWS tanks level the cooling load and heating demand, they prevent the rise of generator temperature. Further, the CWS tanks in the system S_2 reduce the absorber/condenser temperature that enables to lower the generator temperature as well. As a result, the system S_2 obtains the lowest generator temperature. Systems S_0 and S_1 have closer temperatures profiles that mean the factor that significantly lowers the generator temperature is the cooling water temperature and not the load-leveling action using cold tanks. As expected, the integrated CHWS tanks do not affect the temperature of the hot storage temperature. However, the CWS tanks effect it. The hot tank temperature in the S_2 system is 15°C lower on average compared with S and S_1 systems for Izmir. This is a direct consequence of the lower generator temperature. All three systems for Phoenix have nearly the same average hot tank temperature. The reason explaining the similarity of hot tank temperatures of Phoenix is that the DNI value of Phoenix is 80% higher than Izmir as seen from Table 1 and it causes the collector reaches the saturation output temperature more often. Since the load is identical for both locations, there is more heat accumulation in the hot tank in Phoenix compared to Izmir.

Regardless of the systems, the solar heat and boiler heat profiles follow closely each other for locations as it can be seen in Figure 6. Since the DNI values differ based on the locations, the magnitude of the solar heat is higher and boiler heat is lower for Phoenix compared with Izmir. The average solar heat is 245 kW for Izmir and 361 kW for Phoenix. For boiler heat, these values are 160 and 43 kW. The addition of storage tanks to the proposed systems has a negligible effect on the amount of harvested solar energy. However, when it comes to heat loss, the reference system S_0 offers the least heat loss compared with the proposed systems as indicated in Figure 7. The average heat losses increase by 57% and

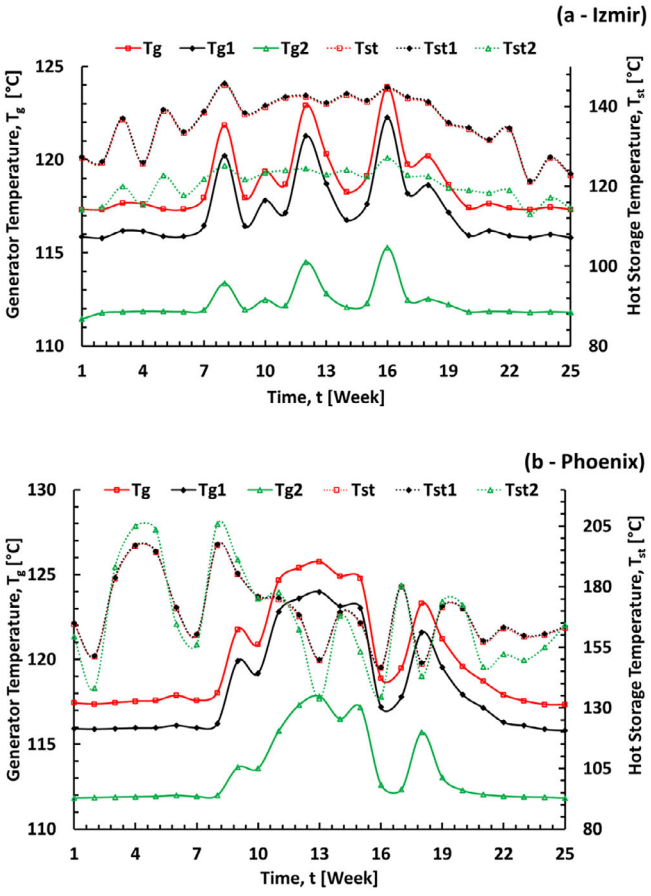

FIGURE 5 Temperature results for Izmir and Phoenix [Colour figure can be viewed at wileyonlinelibrary.com]

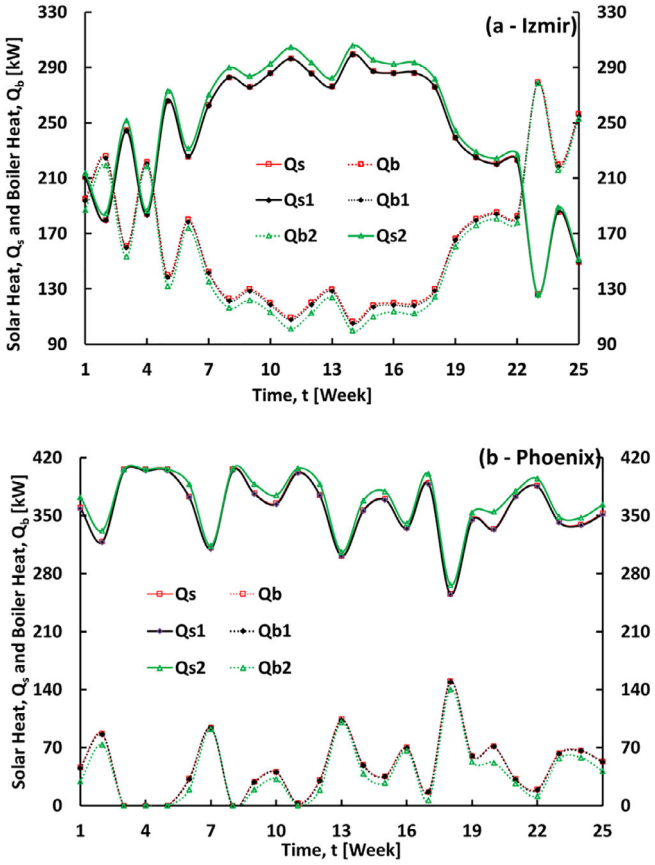

FIGURE 6 Heat power results for Izmir and Phoenix [Colour figure can be viewed at wileyonlinelibrary.com]

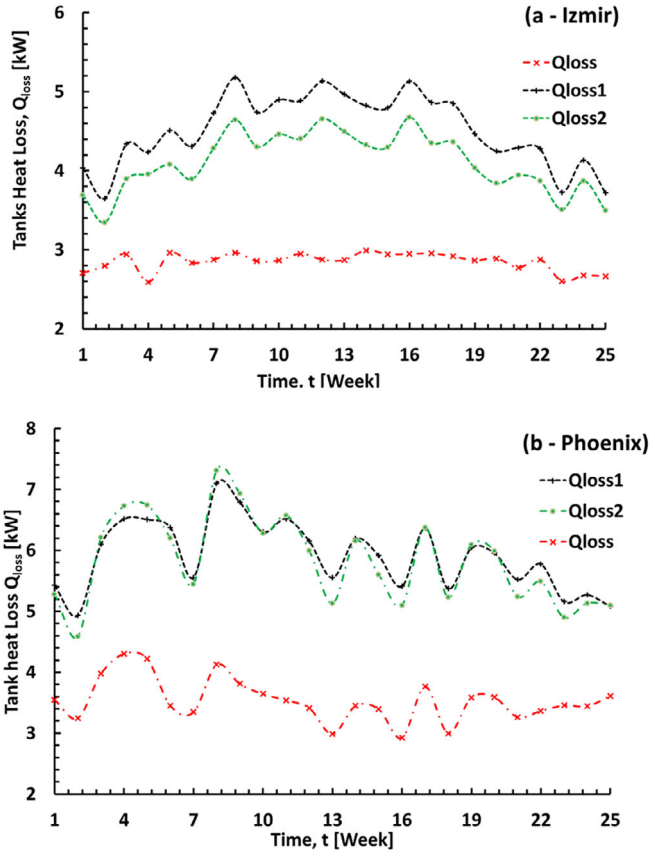

FIGURE 7 Heat loss results for Izmir and Phoenix [Colour figure can be viewed at wileyonlinelibrary.com]

66% for Izmir and Phoenix, respectively. This is mainly due to the heat gain of the CHWS. Phoenix higher ambient temperature leads to higher heat loss.

Figure 8 shows the collector efficiency (η), the solar fraction (sf), and the SPR of three cooling systems for both locations. The results indicate that regardless of the location and system modification, the thermal performances are negligibly affected. The results show that the average collector efficiencies are 44.7% for Izmir and 47.2% for Phoenix. Despite the higher operating temperature of Phoenix, its efficiency is greater than Izmir. This result is due to the low value of the collector efficiency function coefficient (a_2 = 0.0013) that reduces significantly the receiver heat loss. The solar fractions of three systems are simulated and the values are close to each other for Phoenix; however, it drops by 14% for Izmir compared with that of the reference system. For systems performance ratio that is defined as the "COP" of the systems, the system modifications and locations do not affect much and the values remain almost the same with the negligible differences.

From the temperature results, the generator temperatures and hot storage temperatures are close to each other for systems S_0 and S_1; however, S_2 results are smaller. Furthermore, heat performance and seasonal performance values are not changing much with system modifications. In addition to these results, even system S_2 has slightly better results; since the S_1 system has the least modification (the least initial cost), it is considered for system sizing optimization. Figures 9 and 10 show cold storage size, heat loss, chiller peak power, and its CF variation vs the chiller operation hour per day from 10 to 24 hours for the whole season. For all chiller operation duration, the building load remains 14 h/day (from 9:00 to 23:00). Figure 9 shows the effect of chiller operation duration on the heat loss ratio and CHWS tank volume ratio. It can be deduced from the results that when the cooling load ON time (14 h/day) is the same with the chiller ON time, the CHWS volume is minimum. It means the cooling system needs to store chilled water for later use is diminished. As the chiller ON time is shifted by more or fewer operation hours relative to the load time, the cooling system needs for stored chilled water and the volume of the storage tank increases. Heat gain or loss of storage tanks is proportional to their sizes and water storage durations. As heat gain increases, it means the storage duration is the dominating factor in shaping

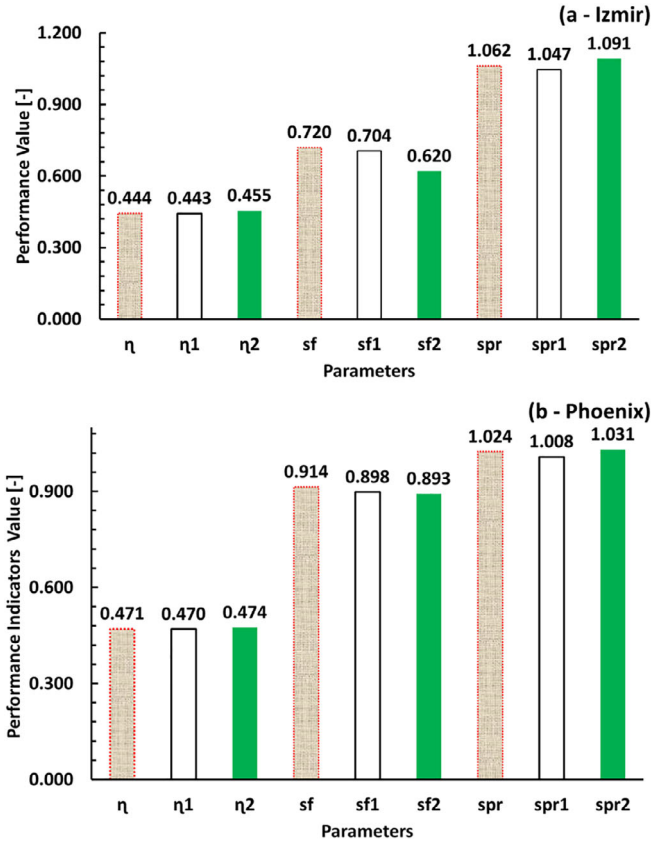

FIGURE 8 Seasonal performance indicators [Colour figure can be viewed at wileyonlinelibrary.com]

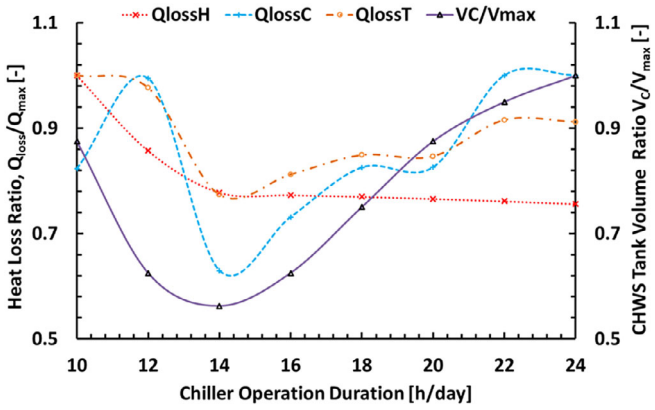

FIGURE 9 S_1 system optimization (tank, volume, and heat loss) [Colour figure can be viewed at wileyonlinelibrary.com]

heat loss profile. Since the tank volume decreases while storage duration increases, the cold tank heat gain increases from 10 h/day operation time to 12 h/day. However, the heat gain decreases from 12 to 14 h/day. The heat gain increases after 14 to 24 h/day because both factors are causing heat loss to increase. In the first section of the curve, the effect of tank volume decreases while that of storage duration increases. As heat gain increases, it means storage duration is the dominating factor. In the second section, tank size reduction is the dominating factor. In

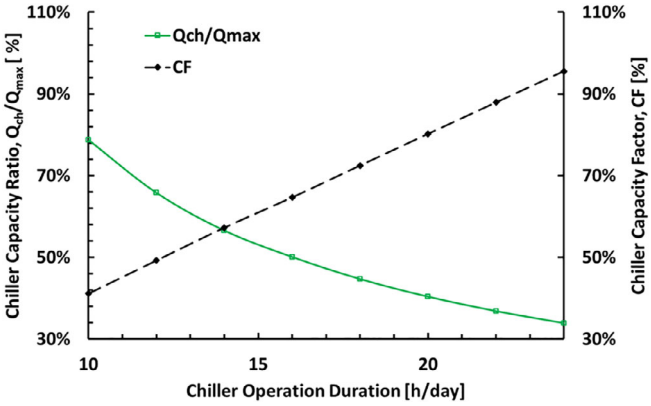

FIGURE 10 S_1 system optimization (chiller, size, and capacity factor) [Colour figure can be viewed at wileyonlinelibrary.com]

the last section, both factors are causing heat loss to increase. Additionally, shorter chiller ON time leads to greater heat loss due to higher operating temperature for the hot tank. When the operation time is extended, hot water does not remain in the hot tank for a long time that reduces heat loss. The total normalized heat loss is lowest for shorter operation time and then slightly increases for longer operation time. Additionally, the required peak power of the chiller decreases almost linearly from 79% at 10 h/day to 34% at 24 h/day for S_1 system as shown in Figure 10. The slight nonlinearity is due to the need of the chiller to support the extra heat loss caused by CHWS tanks. The CF of the chiller increased from 41% to 96% when ON time goes from 10 to 24 h/day as a result of the rated power reduction. Despite the compensation of heat loss caused by storage tanks, it performs much better than the reference system in term of CF improvement.

5 | CONCLUSION

The thermal storage tanks integrated into the solar-powered absorption chiller cooling system was introduced, and the effects of thermal storages and the local irradiation on the system were analyzed. The location influences the solar fraction more compared to tanks addition. The DNI of Phoenix is 80% more than Izmir, and the solar fraction at Phoenix is 28% more compared with Izmir. This result is obtained because of the 250°C cut off output temperature set by the collector manufacturer that does not allow Phoenix to fully harvest the potential solar energy.

By increasing the chiller operation hours per day for model S_1, the required peak power of the chiller is reduced down to 34% of its current value (1020 kW vs 347 kW), driving up the CF from 41% up to 95%. As a result, the

operation cost, including electricity cost and maintenance cost, can be reduced with a much smaller chiller.

The study revealed that the change of the overall thermal performance of the cooling system including the collector efficiency, the solar fraction, and the SPR remain negligible when CHWS tanks are added to level the load. Model S_2 can provide a lower cooling water temperature through night cooling at a reduced water flow rate. However, the lowest cooling water temperature is limited to 20°C to prevent crystallization. This issue does not allow model S_2 to fully show its potential. For applications such as condenser cooling for an electric chiller or for a power plant, which does not have cooling water temperature limitation, model S_2 will show a performance improvement capability.

ORCID

Kasim Toprak https://orcid.org/0000-0002-0043-2941

REFERENCES

1. Cao X, Dai X, Liu J. Building energy-consumption status worldwide and the state-of-the-art technologies for zero-energy buildings during the past decade. *Energ Buildings*. 2016 Sep;128:198-213.
2. Balta MT, Dincer I, Hepbasli A. Performance and sustainability assessment of energy options for building HVAC applications. *Energ Buildings*. 2010;42(8):1320-1328.
3. Cetin KS, Kallus C. Data-driven methodology for energy and peak load reduction of residential HVAC systems. *Procedia Eng*. 2016 Jan;145:852-859.
4. Ayhan Demirbas AAH & AAB. The cost analysis of electric power generation in Saudi Arabia. *Energy Sources*. Policy: Part B Econ Planning; 2017:12.
5. IRENA, *Renewable Power Generation Costs in* 2017. International Renewable Energy Agency, Abu Dhabi. 2018.
6. Sharma C, Sharma AK, Mullick SC, Kandpal TC. Cost reduction potential of parabolic trough based concentrating solar power plants in India. *Energy Sustain Dev*. 2018;42:121-128.
7. Cetinay H, Kuipers FA, Guven AN. Optimal siting and sizing of wind farms. *Renew Energy*. 2017 Feb;101:51-58.
8. EIA U. Electric Power Monthly with Data for July 2018. 2018.
9. Oró E, de Gracia A, Castell A, Farid MM, Cabeza LF. Review on phase change materials (PCMs) for cold thermal energy storage applications. *Appl Energy*. 2012;99:513-533.
10. Helm M, Hagel K. Solar heating and cooling system with absorption chiller and latent heat storage—a research project summary. *Energy Procedia*. 2014 Jan;48:837-849.
11. Behi M, Mirmohammadi SA, Ghanbarpour M, Behi H, Palm B. Evaluation of a novel solar driven sorption cooling/heating system integrated with PCM storage compartment. *Energy*. 2018 Dec;164:449-464.
12. P M S, N N, M S. Experimental and numerical investigation on solar parabolic trough collector integrated with thermal energy storage unit. *Int J Energy res*. 2016 Sep;40(11):1564-1575.
13. Somarriba MJ. Chilled water thermal energy storage tank overview [internet]. *DN Tanks*. 2016; Available from: https://bit.ly/2rliqiT.
14. University of Illinois. Thermal Energy Storage [Internet]. 2011. Available from: https://bit.ly/2G23MqQ
15. Boonnasa S, Namprakaib P. The chilled water storage analysis for a university building cooling system. *Appl Therm Eng*. 2010; 30:11-12.
16. Syed A, Izquierdo M, Rodríguez P, et al. A novel experimental investigation of a solar cooling system in Madrid. *Int J Refrig* [Internet. 2005 [cited 2019 Mar 25;28(6):859-871. Available from. https://www.sciencedirect.com/science/article/pii/S0140700705000277.
17. El-Shaarawi MAI, Al-Ugla AA. Hybrid storage designs for continuous operation of solar-powered LiBr-water absorption air-conditioning. *Int J Energy Res* [Internet. 2016 May;40(6): 791-805.
18. Yan C, Wang S, Fan C, Xiao F. Retrofitting building fire service water tanks as chilled water storage for power demand limiting. *Build Serv Eng res Technol*. 2017 Jan;38(1):47-63.
19. Sebzali MJ, Ameer B, Hussain HJ. Ecomomic assessment of chilled water thermal storage and conventional air-conditioning systems. *Energy Procedia*. 2012;18:1485-1495.
20. Lin H, Li X, Cheng P, Xu B. Study on chilled energy storage of air-conditioning system with energy saving. *Energ Buildings*. 2014 Aug;79:41-46.
21. Rosiek S, Javier F. Performance evaluation of solar-assisted air-conditioning system with chilled water storage (CIESOL building). *Energ Conver Manage*. 2012;55:81-92.
22. Zhu K, Li X, Campana PE, et al. Techno-economic feasibility of integrating energy storage systems in refrigerated warehouses. *Appl Energy*. 2018;216:348-357.
23. CANBAY ÇS. Optimization of HVAC Control Strategies By Building Management Systems Case Study: Özdilek Shopping Center. 2003.
24. TRNSYS. Mathematical reference volume 5. 2006.
25. Morrison G, White S. Multi-effect absorption chillers powered by the sun: reality or reverie. *Energy Procedia*. 2016 Jun;91: 844-856.
26. Weiss W, Rommel M. Process heat collectors. State of the art within Task 33/IV. IEA SHC-Task 33 and SolarPACES-Task IV: Solar Heat for Industrial Processes. 2008
27. Rockwool Ltd. Roll, Twin Roll and Rollbatt. 2014 Available from: http://static.rockwool.com/globalassets/rockwool-uk/downloads/datasheets/floors/roll-datasheet.pdf.
28. Asadi I, Shafigh P, Bin AHZF, Mahyuddin NB. Thermal conductivity of concrete—a review. *J Build Eng*. 2018 Nov;20:81-93.
29. Liu N, Zhang L, Jia X. The effect of the air water ratio on counter flow cooling tower. *Procedia Eng*. 2017;205:3550-3556.
30. Cooling tower. *Energy Efficiency in Electrical Utilities, Bureau of energy efficiency, Ministry of Power, Government of India, New Delphi, India*, [Internet]; 2005 Available from: http://www.emea.org/gbook13.asp.
31. Khamis Mansour M, Hassab MA. Innovative correlation for calculating thermal performance of counterflow wet-cooling tower. *Energy*. 2014 Sep;74:855-862.

How to cite this article: Toprak K, Ouedraogo KE. Effect of storage tanks on solar-powered absorption chiller cooling system performance. *Int J Energy Res*. 2020;44:4366–4375. https://doi.org/10.1002/er.5210